Indonesian. J. Pharm.
Volume 36 Issue 4 (2025)
October-December

ISSN : 2338-9427
Formerly ISSN : 0126-1037

Indonesian Journal of Pharmacy

(*Indonesian J. Pharm.*)

Accredited by DGHE (DIKTI) No. 72/E/KPT/2024

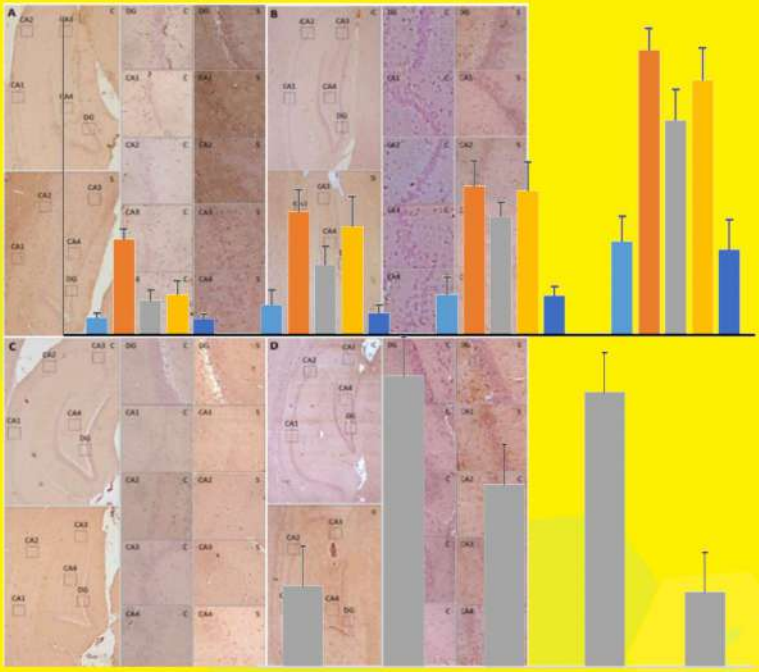

Faculty of Pharmacy
Universitas Gadjah Mada

PUBLISHED: 2025-12-18

REVIEW ARTICLE

Bibliometric Analysis of Research on Herbal Medicine for Inflammation From 2004 to 2023

Alfian Syarifuddin, Arief Nurrochmad, Nanang Fakhrudin

592-610

PDF SUPPLEMENTARY DATA

RESEARCH ARTICLE

Physicochemical Evaluation and Anti-Aging Activity of The Cream Formulation Containing Aloe Vera and Rosella Extracts

Rita Wulandari, Eunike Catherine Chandra, Ines Septi Arsiningtyas, Dwi Ni'maturrohmah, Ade Erma Suryani, Cici Darsih, Sari Haryanti, Nur Maulidah Rahmah, Sri Handayani

611-621

PDF

Formulating of moringa oil microemulsion used Surfactant Poly Ethylene Glycol 40 Hydrogenated Castrol Oil and Co-Surfactant of Glycerin

Uswatun Chasanah, Nining Sugihartini, Sapto Yuliani

622-637

PDF

Hair Serum Nanoemulsion loaded Clove Essential Oil Formulation for Androgenetic Alopecia: Characterization and Hair Growth Activity

Wayan Cintya Ganes Budastra, Teti Mariam Riandari, Laras Novitasari, Retno Murwanti, Ronny Martien

638-645

PDF

Unveiling Metabolite Compounds and Anti-Inflammatory Properties from Chromolaena odorata in Three Geothermal Areas

Nur Balqis Maulydia, Khairan Khairan, Trina Ekawati Tallei, Rinaldi Idroes

646-660

PDF

One-Pot Synthesis and Biological Evaluation of Piperidinium-3,3'-(arylmethylene) bis-lawsone derivatives by targeting caspase-7

Elvira Hermawati, Muhammad Taufik, Ade Danova, Warinthorn Chavasiri, Didin Mujahidin

661-670

PDF

Abstract views: 278 | views: 75

Evaluating the Impact of a Modified UCMS Protocol with a Psychological Stress Device on Neurobiological and Behavioral Responses in Rats

Ivonne Soeliono, Lannie Hadisoewignyo, Ika Puspitasari, Andayana Puspitasari Gani, Yudy Tjahjono, Gladdy L. Waworuntu, Britney Chelsea Brigitta Mandagie, I Made Agus Permana Putra, Gracelia Suhandri, Detika Aksamina Jumina Tulimau, Ignatia Putri Febriana Yulianto, Fitria Nuraini, Rachmadani Sya'adillah, Dyana Linggar Swari

671-684

PDF

Abstract views: 492 | views: 78

Computer-aided Discovery of Bioactive Natural Product Isoliquiritigenin as an Acetylcholinesterase Inhibitor

Stephanus Satria Wira Waskitha, Enade Perdana Istyastono, Michael Raharja Gani, Florentinus Dika Octa Riswanto

685-694

PDF SUPPLEMENTARY DATA

Abstract views: 398 | views: 91 views: 15

Lipid Peroxidation Inhibition of Three Choline Chloride-based NADES Extracts from Pluchea indica Leaves: Ex vivo and in silico Approach

Ni Putu Ermi Hikmawanti, Tahyatul Bariroh, Agustin Yumita, Fadlina Chany Saputri, Arry Yanuar, Abdul Mun'im, Labibah Zikriyah, Aisyah Nur Fitriyani, Rini Mulyati, Lathifah As'ad Dzulnia Sekar

695-708

PDF SUPPLEMENTARY DATA

Abstract views: 196 | views: 65 views: 16

Evaluation of Adherence to Prescription Guidelines for Secondary Prevention at Discharge Following Ischemic Stroke

Ola Ali Nassr, Paul Forsyth, Huda Muhammed Muzher, Raghad Faris Wadeea, Sara Delman Najim, Aya Manhal Mustafa, Mustafa Shaalan Tarish

709-719

PDF

Abstract views: 225 | views: 70

Survey of Bachelor of Pharmacy Students Thesis Trends Before, During, and After the Covid-19 Pandemic

Muhammad Royyan Alfatah, Anna Wahyuni Widayanti, Arief Rahman Hakim, Agung Endro Nugroho

720-730

PDF

Abstract views: 232 | views: 75

New, Valid, and Reliable Indonesian Version of the Quality of Life Assessment Instrument Based On the Health Condition: Health-Related Quality of Life With Six Dimensions

Imaniar Noor Faridah, Dyah Aryani Perwitasari, Haafizah Dania, Mohammad Adam Bujang

731-741

PDF

Determinant of Smoking Cessation Behavior among Low Dependence Smokers: A Discrete Choice Experiment

Eliza Dwinta, Susi Ari Kristina, Vo Quang Trung

742-752

Health Impact of Unauthorized Medicine Sales in an Industrial Distribution Center

Parun Rutjanathamrong, Wisood Siripattanakulkajorn, Pansa Phorntrakoonpakdee, Chaoncin Sooksriwong, Tuangrat Phodha

753-764

Knowledge of Intravenous Preparation among Health Professionals and Assessment of the Sterile Product Label Information Coverage

Erna Prasetya Ningrum, Fita Rahmawati, Endang Lukitaningsih, Marlyn Dian Laksitorini

765-776

In Vitro Evaluation of 4-Methoxyresorcinol and Kaempferol 7-ORutinoside and Their Radioiodinated Derivatives in MCF-7, MDA-MB-231, and LNCaP Cell Lines

Hendris Wongso, Putri Rochmantika , Alfian M. Forentin, Veronika Y. Susilo , Muhamad B. Febrian , Isa Mahendra , Ahmad Kurniawan , Crhisterra E. Kusumaningrum, Asep Rizaludin , Yanuar Setiadi, Ari S. Nugraha

777-787

Factors Affecting Preparation of Repaglinide Nanoparticles for Dissolution Improvement

Hamsa Yaseen Ghadhan, Kawther Khalid Ahmed

788-800

Editorial Policies
Instructions for Authors
Article Processing Charge
Peer Review Process
Indexing & Archiving
Journal Statistics
Journal History
Editorial Office
Article In Press
Publication Process
Template Document
Gen AI Policy

INFORMATION

For Readers
For Authors
For Librarians

MOST READ LAST WEEK

Digital Health Literacy and Its Associated Factors in General Population in Indonesia
830

Anti-Acne Mushrooms: A Review
728

Validation of UV-Vis Spectrophotometric Method to Determine Drug Release of Quercetin Loaded-Nanoemulsion
653

Design and Evaluation of The Floating Oral In Situ Gelling System of Levofloxacin Hemihydrate to Dysphagia Patients
618

Optimization of HPMC and Carbopol 940 as Gelling Agents on The Physical Properties and Stability in Anti-Acne Gel of Binahong Leaves (Anredera cordifolia (Ten.) Steenis Extract
567

CURRENT ISSUE

Editorial Office:
FACULTY OF PHARMACY
UNIVERSITAS GADJAH MADA
Jl. Kaliurang Km.4 Sekip Utara
Yogyakarta 55281

Indonesian Journal of Pharmacy is indexed by :
SCOPUS, DIMENSION, Google Schoolar, SINTA, DOAJ

Editor In Chief

Editorial Board

Indonesian Journal of Pharmacy

VOL 36 (4) 2025: 685–694 | RESEARCH ARTICLE

Computer-aided Discovery of Bioactive Natural Product Isoliquiritigenin as an Acetylcholinesterase Inhibitor

Stephanus Satria Wira Waskitha[1], Enade Perdana Istyastono[2,3], Michael Raharja Gani[1] and Florentinus Dika Octa Riswanto[1]*

[1] Research Group of Computer-Aided Drug Design and Discovery of Bioactive Natural Products, Faculty of Pharmacy, Sanata Dharma University, Yogyakarta 55282, Indonesia
[2] Research Center for Cheminformatics and Molecular Modeling, Atma Jaya Catholic University of Indonesia, Jl. Pluit Raya No. 2, Jakarta Utara, DKI Jakarta, 14440, Indonesia;
[3] Department of Pharmacy, School of Medicine and Health Sciences, Atma Jaya Catholic University of Indonesia, Jl. Pluit Raya No. 2, Jakarta Utara, DKI Jakarta, 14440, Indonesia

Article Info

Submitted: 21-09-2024
Revised: 06-02-2025
Accepted:24-02-2025

*Corresponding author
Florentinus D.O. Riswanto

Email:
dikaocta@usd.ac.id

ABSTRACT

Bioactive natural products have been extensively investigated for the discovery of alternative Alzheimer's disease (AD) treatments. Recently, our structure-based virtual screening (SBVS) campaigns on natural products served in the LOTUS database exhibited the potency of isoliquiritigenin as an acetylcholinesterase (AChE) inhibitor, which propelled us to investigate it further. This study aimed to evaluate the acetylcholinesterase (AChE) inhibitory activity of isoliquiritigenin compared to commonly known inhibitors, i.e., donepezil, through in vitro and in silico studies. The AChE inhibitory activity of isoliquiritigenin and donepezil was evaluated using the improved Ellman method, and the molecular mechanism for inhibiting AChE was identified using molecular docking and dynamics simulations. Our findings verified the AChE inhibitory activity of isoliquiritigenin, possessing an IC_{50} value of 126.22 µM compared to donepezil, with an IC_{50} value of 36.98 µM. In silico studies revealed that five best-docked poses from 100 redocking and molecular docking simulations established interactions in the AChE active site in 5 ns after 5-ns equilibration run. Further dynamics interactions were explored to 50 ns, showing interactions of isoliquiritigenin and donepezil, which were still in the AChE active site. These simulations also revealed the pivotality of the aromatic ring and hydroxyl moiety of isoliquiritigenin reinforcing the receptor-ligand stabilization. Hence, our studies exhibited the potency of isoliquiritigenin acting as an AChE inhibitor and might be explored in isoliquiritigenin-containing bioactive natural products as AD alternative treatments.

Keywords: Acetylcholinesterase Inhibitor, Isoliquiritigenin, In Vitro Study, In Silico Study, Natural Products

INTRODUCTION

Recently, we performed structure-based virtual screening (SBVS) campaigns on 276,518 natural products from the LOTUS database to discover acetylcholinesterase (AChE) inhibitors. From 867 compounds identified as virtual hits, we found that among them was isoliquiritigenin (Riswanto et al., 2024). Hence, this research aimed to examine the AChE inhibitory activity of isoliquiritigenin, which was previously discovered in our SBVS campaigns.

Isoliquiritigenin, a type of chalcone derivative, was extensively investigated to have various pharmacological properties such as counteracting oxidative stress (Dong et al., 2024), neuroprotective (Shi et al., 2020), anticancer (Wang et al., 2021), and antidiabetic activity (Gaur et al., 2014). This compound was also found in many foods, beverages, (Zhang et al., 2010) and in the leaves of *Muntingia calabura,* i.e., a plant abundantly spread in many countries, especially in Indonesia (Mahmood et al., 2014).

A study revealed that the ability of drugs to cross the blood-brain barrier (BBB) is a pivotal consideration for drugs treating neurodegenerative diseases. As expected,

isoliquiritigenin was able to penetrate the blood-brain barrier (BBB) and distribute within brain tissue, as reported in the previous literature (Li et al., 2015; Ramalingam et al., 2018; Wang et al., 2021). Still, the investigation of isoliquiritigenin in inhibiting AChE remains rarely explored nowadays, which also supports our research in evaluating the AChE inhibitory activity of isoliquiritigenin.

Over time, Alzheimer's disease (AD) has been highlighted as a public health concern, and AD incidence is predictably projected to increase in 2050 (Nichols et al., 2022). In recent years, developing natural products-based AD treatments has been a significant concern to overcome this incidence (Gajendra et al., 2024). Indeed, the explorations of plant-derived compounds and bioactive natural products have been widely accentuated as potential alternative AD treatments since they possess therapeutic benefits with relatively fewer adverse effects (Ahmed et al., 2021; Gajendra et al., 2024), propelling us to investigate the potency of isoliquiritigenin as an abundantly-found natural product.

This research evaluated the AChE inhibitory activity of isoliquiritigenin discovered from our SBVS campaigns (Riswanto et al., 2024) based on the improved Ellman method, as previous studies utilized this in vitro method (Hafiz et al., 2020; Ketenci et al., 2020). To study the molecular mechanism of isoliquiritigenin interacting in the AChE active site, 100 molecular docking followed by molecular dynamics (MD) simulations and interaction hotspots identification were implemented to provide in silico perspective. These findings could serve the potency of isoliquiritigenin as an AChE inhibitor to encourage the discovery of bioactive natural products as alternative AD therapies.

MATERIALS AND METHODS

Chemicals

Isoliquiritigenin (CAS No: 961-29-5) and donepezil hydrochloride (CAS No: 120011-70-3) were purchased from Sigma-Aldrich (St. Louis, MO, USA). QuantiChrom™ Acetylcholinesterase Inhibitor Screening Kit (DACE-100) was also purchased from BioAssay Systems (Hayward, CA., USA). Dimethyl sulfoxide (DMSO) (Cas No: 67-68-5) was used as the solvent and was purchased from Sigma-Aldrich (St. Louis, MO, USA).

In Silico Instrumentation

The molecular simulations studies, including molecular docking and dynamics simulations, were performed on a personal computer. This computer was equipped with an AMD Ryzen 7 5800X processor, an NVIDIA GeForce GTX 1650 graphics card, 32GB of RAM, and a 466 GB solid-state drive. This computer was also integrated with YASARA-Structure 24.4.10 with our in-house developed plug-in to perform 100 redocking simulations as well as molecular docking simulations and PyPLIF HIPPOS 0.2.0 to identify interactions hotspots from MD simulations (Istyastono et al., 2023; Waskitha et al., 2023).

Acetylcholinesterase Inhibitory Assay

The acetylcholinesterase inhibitory activity of the tested compounds, i.e., isoliquiritigenin and donepezil as the positive control, was evaluated using the improved Ellman method. A series of isoliquiritigenin and donepezil solutions was prepared with DMSO as the solvent at 500, 200, 100, 50, and 0 µM concentrations. The acetylcholinesterase inhibitory activity of the tested compounds was evaluated according to the manufacturer's protocol. This assay kit contains assay buffer (pH 7.5), calibrator, and reagent. The working reagent was freshly prepared by dissolving the reagent with assay buffer with a concentration of 2 mg/200 µL.

The calibrator and DMSO were used in a different well of clear 96-well plate (200 µL). In the separate well, the tested compound solution (10 µL) was mixed with the working reagent (190 µL). Instead of optical density, the absorbance was calculated at 2 and 10 minutes in the plate reader using Synergy HTX-3 multimode reader (at 412 nm wavelength) integrated with Gen5 3.08 software. The absorbance calculation was conducted at 25 °C. Finally, acetyl-cholinesterase activity was calculated using this equation as follows:

$$\text{AChE Activity} = \frac{\text{Abs}_{10} - \text{Abs}_{2}}{\text{Abs}_{\text{cal}} - \text{Abs}_{\text{DMSO}}} \times 200\ (U/L)$$

Based on the equation, Abs_{10} and Abs_{2} were the absorbance values of the tested compound at 10 and 2 minutes, respectively. The absorbance of the calibrator and DMSO at 10 minutes was denoted by Abs_{cal} and Abs_{DMSO}. The number "200" is the equivalent activity of the calibrator under the assay conditions as mentioned in the manufacturer's protocol. The AChE activities measured were then converted to inhibition percentage to obtain the IC_{50} value of the tested compounds. The absorbance measurements were performed in triplicate for all wells, except the

isoliquiritigenin solutions at 50 μM concentration, which were measured in duplicate.

Receptor-Ligand Preparation

Receptor-ligand preparation was initiated before conducting redocking and docking simulations. This preparation was based on our previous research (Istyastono et al., 2023; Waskitha et al., 2023). As YASARA-Structure could directly download the receptor-ligand complex, this research used a three-dimensional model of human acetylcholinesterase complexed with donepezil as the native ligand (PDB ID: 7E3H). This research selected chain A (mol A) as the studied model in this model.

To obtain the complete structure of the receptor, the missing amino acids were built into the receptor model. The removal of other insignificant molecules i.e., water, Nag, and Fuc molecules was done followed by the addition of the terminal cap of the receptor. The system was further prepared by adjusting its pH to 7.4 to mimic physiological conditions, structure checking, and energy minimization. The corrected structure was then saved as 7e3h-corr-min.yob for further simulations.

Redocking Simulations of Donepezil

In this research, 100 redocking simulations were performed using our in-house developed plug-in as previously published (Istyastono et al., 2023; Waskitha et al., 2023). This plug-in allowed us to perform 100 redocking simulations of the native ligand and resulted in redocked poses in a different working directory for each n^{th} simulation. The root mean square deviation (RMSD) value was calculated based on the superimposition of the best-redocked native ligand from each simulation to its crystallographic structure according to 7e3h-corr-min.yob. The RMSD values were considerably accepted if the values were ≤ 2.000 Å of 95% of all the best-redocked poses. Therefore, the redocking protocol could be used for molecular docking simulations of isoliquiritigenin (Diallo et al., 2021; Istyastono et al., 2023).

Molecular Docking Simulations of Isoliquiritigenin

This research also utilized our in-house developed plug-in as recently conducted in our previous research (Istyastono et al., 2023; Waskitha et al., 2023). To perform 100 molecular docking simulations with the same configuration as the redocking simulations. The resulting files from redocking simulations, i.e., MacroTarget_receptor.sce and MacroTarget_config.mcr, were duplicated in another directory in which 100 molecular docking simulations of isoliquiritigenin were performed.

Using YASARA-Structure, the three-dimensional structure of isoliquiritigenin was built using its SMILES code i.e., O=C(/C=C/C(=CC=C1O)C=C1)C(=CC1)C(O)=CC=1O. The system pH was set to 7.4 as the physiological conditions followed by structure checking and energy minimization, respectively. The structure was then saved and selected as the MacroTarget to perform 100 molecular docking simulations.

These simulations generated RMSD value of the best-docked pose of isoliquiritigenin, which was generated from the superimposition of the best-docked pose from each simulation to the best-docked pose from the first simulation. Hence, the best-docked pose with RMSD value of > 2.000 Å noticeably had a different pose compared to the best-docked pose from the first simulation (Istyastono et al., 2023; Waskitha et al., 2023).

Molecular Dynamics Simulations

Molecular dynamics (MD) simulations were also carried out using YASARA-Structure and aimed to evaluate the dynamics interactions of docked native ligand and isoliquiritigenin. The simulations were configured using YASARA-Structure md_run.mcr macro file, as mentioned in the previous research (Istyastono et al., 2023).

The AMBER14 forcefield was used to model atomic interactions and the periodic boundary conditions were implemented. The system was enclosed in a cubic cell with an extension of the cell 10 Å around all atoms. In the system, water molecules were selected as the solvent with the density of 0.993 g/mL, with the temperature of 310 K, and the pressure of 1 bar. The Na^+ and Cl^- ions were added as mimicking physiological conditions with a concentration of 0.9%. Particle Mesh Ewald method was employed for long-range coulomb force calculations without a cutoff, while van der Waals forces had a cutoff of 8.000 Å.

Before running MD simulations, the system underwent energy minimization using the steepest descent followed by simulated annealing methods to reduce steric clashes. The MD simulations then ran for 15 ns simulation, with the first 5 ns as the equilibration run followed by 10 ns production run. The production run was prolonged to 40 ns to explore the dynamics interaction further. Hence, the total MD simulations time was 50 ns. The MD

simulations were run using 2.5 fs timesteps, and the snapshots were taken every 100 ps.

The MD simulations were performed with five replications for each receptor-ligand complex obtained from each of the best-redocked and docked with the lowest free energies of binding (FEB) (Liu et al., 2017; Liu & Kokubo, 2017). For each complex, the simulations produced RMSD values for the receptor's backbone atoms (RMSD-Backbone) and the ligand movement (RMSD-Ligand Movement) at each saved snapshot. Changes in these RMSD values were analyzed to evaluate conformational stability.

Free Energies of Binding Evaluation

The FEB for each snapshot from the MD simulations was computed using a YASARA-Structure macro called md_analyzebindingenergy.mcr. This macro employed the AMBER14 force field, maintaining consistency with the force field used in the MD simulations. The Poisson-Boltzmann (PBS) method was applied at 310 K to calculate solvation energy. The FEB calculation was performed using the VINA local search (VINALS) algorithm.

Interaction Hotspots Analysis

This research employed PyPLIF HIPPOS 0.2.0 to analyze interaction hotspots from each MD snapshot, utilizing the direct IFP feature as in our recently published research (Istyastono et al., 2023). Snapshots from MD simulations were converted to PDB format using a YASARA macro file (md_convert.mcr), excluding water molecules. The software analyzed interactions in each snapshot and then grouped them by type to pinpoint interaction hotspots throughout the MD simulations.

RESULTS AND DISCUSSION

Acetylcholinesterase Inhibitory Assay

The inhibitory activity of isoliquiritigenin and donepezil against AChE was well assessed using the improved Ellman method. The thiocholine produced by the AChE enzymatic reaction reacted with 5,5'-dithiobis(2-nitrobenzoic acid), resulting in the product of a yellow-colored compound. The product's intensity was proportionally to the AChE activity in the sample. The inhibition percentages of isoliquiritigenin and donepezil against AChE were derived from the obtained AChE activity (Figure 1). Donepezil exhibited a better inhibitory effect than isoliquiritigenin at concentrations of 50, 100, and 200 μM. However, at a concentration of 500 μM, the inhibitory activity of isoliquiritigenin appeared to surpass donepezil. At a concentration of 500 μM, isoliquiritigenin showed a slightly higher inhibition percentage compared to donepezil, suggesting that at higher concentrations, isoliquiritigenin might provide better AChE inhibitory activity. According to our findings, the obtained IC_{50} of isoliquiritigenin and donepezil was 126.22 and 36.98 μM, respectively.

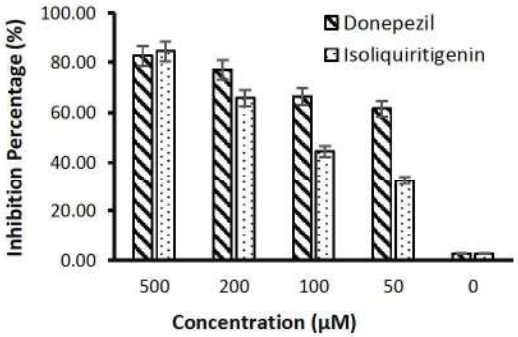

Figure 1. The percentage of AChE inhibition by isoliquiritigenin and donepezil

Compared to the commonly available AChE inhibitor i.e., donepezil, isoliquiritigenin possessed the lower inhibitory activity. Even so, it was discovered that isoliquiritigenin inhibited AChE with the lower IC_{50} value compared to other natural products such as morusinol, i.e., flavonoid compound isolated from the root bark of *Morus lhou L* (IC_{50} = 173.49 μM) (Kim et al., 2011) and certain flavonoids from *Paulownia tomentosa* fruits, i.e., hesperetin (IC_{50} = 2476.1 μM), naringenin (IC_{50} = 2045.0 μM), and eriodictyol (IC_{50} = 1663.8 μM) (Cho et al., 2012). Interestingly, our findings exhibited that isoliquiritigenin possessed better AChE inhibitory activity than another widely-studied flavonoid compound, i.e., quercetin (IC_{50} = 353.86 μM) (Khan et al., 2009).

Our studied compound also had a better AChE inhibitory activity than certain alkaloid compounds reported in previous literature review (Konrath et al., 2013). Our results might serve the potency of isoliquiritigenin as an AChE inhibitor for alternative AD treatment. To comprehend the molecular inhibitory mechanism of both isoliquiritigenin and donepezil against AChE, molecular docking and dynamics simulations were subjected to give in silico perspectives.

Molecular Docking Simulations

Initially, 100 redocking simulations were performed to validate the proposed molecular docking protocol. The results showed that RMSD values of best-redocked donepezil were ranged from 0.311 to 0.550 Å with an average value of 0.407 Å, suggesting that the molecular docking protocol was valid, allowable, and, therefore, could be used to dock isoliquiritigenin with the same protocol (Diallo et al., 2021; Istyastono et al., 2023; Waskitha et al., 2023). The best-redocked donepezil had FEB of -12.310 to -12.451 kcal/mol, possessing an average FEB of -12.381 kcal/mol. In both redocking and molecular docking simulations, the lower value of FEB indicated the more favorable docked pose. The representative of the best-redocked pose with the lowest FEB value of -12.451 kcal/mol was conformationally stabilized by predominantly aromatic and hydrophobic interactions with the active site amino acid residues.

The best-docked isoliquiritigenin interacted in the AChE active site with FEB values ranging from -9.566 to -9.673 kcal/mol. Interestingly, these simulations produced best-docked isoliquiritigenin with all RMSD values of ≤ 2.000 Å with a maximum value of 0.113 Å, indicating that there was only one dominant best-docked pose result. As predicted, the best-docked pose with the lowest FEB value formed aromatic interactions due to the aromatic features of isoliquiritigenin.

To ensure the conformational stability of the resulted best-docked pose, previous research encouraged the redocking as well as molecular docking results to be validated further with MD simulations (Chen, 2015). In this research, the conformational stability of the ligand in the AChE active site was assessed based on the top five lowest FEB values of the best-docked pose from redocking and docking simulations. This research revealed that the native ligand produced the top five best-redocked poses with FEB values of -12.451 (DNP-1), -12.447 (DNP-2), -12.447 (DNP-3), -12.444 (DNP-4), and -12.441 (DNP-5) kcal/mol whereas isoliquiritigenin produced best-docked poses with FEB values of -9.673 (ISL-1), -9.672 (ISL-2), -9.671 (ISL-3), -9.671 (ISL-4), and -9.670 (ISL-5) kcal/mol, respectively. All redocking and molecular docking results, i.e., FEB values and interacting amino acid residues, are provided (Supplementary File 1). In addition, visualization of the best-redocked pose and the best-docked pose compared to the end of 10 ns MD simulations pose is also presented (Supplementary File 2).

Molecular Dynamics Simulations

Conformational stability and dynamics interactions of isoliquiritigenin and donepezil were graphically evaluated from the final snapshot of equilibration run (5 ns) to 10 ns. The graph depicting conformational stability evaluation from the top five best-docked conformations ranked from the lowest to highest FEB value is colored with red (DNP-1 and ISL-1), yellow (DNP-2 and ISL-2), green (DNP-3 and ISL-3), blue (DNP-4 and ISL-4), and purple (DNP-5 and ISL-5), respectively. The red-colored graph indicates the lowest FEB value, while the purple-colored graph indicates the highest FEB value from the top five best-redocked and best-docked poses.

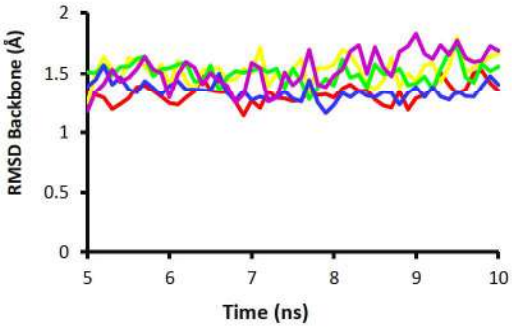

Figure 2. The dynamics conformational changes of AChE backbone atoms of DNP-1 (red), DNP-2 (yellow), DNP-3 (green), DNP-4 (blue) and DNP-5 (purple) complex

The conformational stability evaluation in changes of the RMSD Backbone atoms of AChE was also examined (Figure 2). Our results exhibited that at the initial conformation of the simulations, starting from 0 ns at the equilibration run, the RMSD Backbone gradually increased with RMSD Backbone of ≤ 2.000 Å. After 5 ns, it was observed that all donepezil complexes (DNP-1 to DNP-5) still maintained RMSD Backbone atoms value of ≤ 2.000 Å, exhibiting the conformational stability of the receptor backbone atoms after the equilibration run until 10 ns MD simulations.

Interestingly, the DNP-3 complex maintained the donepezil conformational stability in the AChE active site from 5 to 10 ns production run with RMSD Ligand Movement of ≤ 2.000 Å (Figure 3). Our research found that although the conformation of AChE backbone atoms of complex DNP-1, DNP-2, DNP-4, and DNP-5 was stable, there were several observable RMSD Ligand Movement of > 2.000 Å. Nonetheless, donepezil still interacted

in the AChE active site at these snapshots, according to our visual inspections.

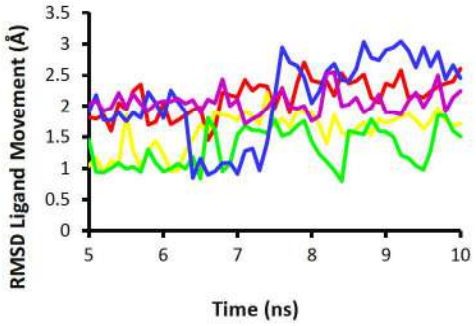

Figure 3. The dynamics conformational changes of donepezil interacting with amino acid residues of AChE colored with red (DNP-1), yellow (DNP-2), green (DNP-3), blue (DNP-4), and purple (DNP-5)

From 5 to 10 ns MD simulations, PyPLIF HIPPOS 0.2.0 recognized several interaction hotspots, such as hydrogen bonds, aromatic, and hydrophobic interactions. Although there were many observed hydrophobic interactions, those interactions are not listed in this work since all amino acid residues in the AChE active site could form hydrophobic interactions (Windah & Istyastono, 2024). All interaction hotspots of donepezil interacting in the AChE active site during 5 to 10 ns MD simulations are also tabulated (Supplementary File 3). This analysis revealed that hydrogen bonds and aromatic interactions played a role in AChE-donepezil stabilization. It was examined that the N-benzylpiperidine moiety of donepezil in DNP-1, DNP-2, DNP-4, and DNP-5 complex formed hydrogen bonds with Tyr337 during 5 to 10 ns MD simulations. In addition, aromatic edge-to-face interactions with Tyr341 and Tyr337, as well as aromatic face-to-face interactions with Trp86 and Trp286, are also dominantly established in all donepezil complexes.

Our visual inspections proved that the existence of aromatic and N-benzylpiperidine moiety of donepezil stabilized the receptor-ligand interactions, especially interacting with aromatic amino acid residues. These findings were also well-correlated with previous research, showing the important feature of N-benzylpiperidine moiety to enhance the AChE inhibitory activity (Sugimoto, 1999). Meanwhile, the role of aromatic ring as the important moiety of AChE inhibitors was explained in the previous study (Mohsin & Ahmad, 2020).

This research also revealed that several selected best-docked poses of AChE-isoliquiritigenin complex, i.e., ISL-2, ISL-3, and ISL-5 could maintain the AChE backbone atoms stably, with RMSD value ≤ 2.000 Å along 5 to 10 ns MD simulations. In contrast, ISL-1 and ISL-4 could not maintain the RMSD Backbone atoms value of ≤ 2.000 Å throughout the simulation time, and it could be noticed there were several snapshots possessing RMSD Backbone atoms value of > 2.000 Å (Figure 4). These findings denoted that receptor-ligand complexes with the same FEB value from molecular docking simulation might not produce in similar conformational stability of the examined system.

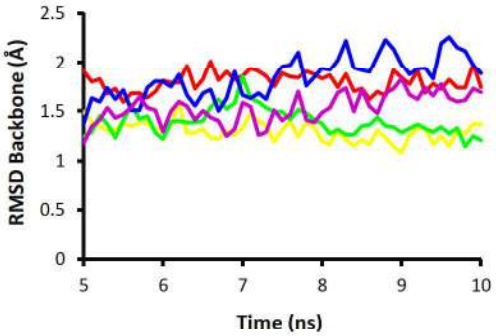

Figure 4. The dynamics conformational changes of AChE backbone atoms of ISL-1 (red), ISL-2 (yellow), ISL-3 (green), ISL-4 (blue) and ISL-5 (purple) complex

From the end of the equilibration run to 10 ns MD simulations, isoliquiritigenin in the receptor-ligand complex of ISL-1 to ISL-5 was noticed to have higher ligand conformational changes than donepezil, as several MD snapshots possessed RMSD ligand movement values of > 2.000 Å (Figure 5). Even if ISL-1 was the best-docked isoliquiritigenin, possessing the lowest FEB value, this complex had the highest RMSD ligand movement value compared to the other complexes. However, in contrast, ISL-5, i.e., best-docked isoliquiritigenin having the highest FEB from the selected top five best-docked poses, possessed the lowest RMSD Ligand Movement values. These MD simulation results revealed that we cannot easily judge the receptor-ligand stability based on the FEB produced from molecular docking results. As mentioned in the previous research, the molecular docking results could be further validated with MD simulations to avoid questionable docking results (Chen, 2015).

Even if several MD snapshots possessed RMSD ligand movement of > 2.000 Å with the highest value of 5.585 Å from ISL-1 complex, isoliquiritigenin still interacted in the AChE active site, forming interactions of aromatic edge-to-face with Tyr124, Trp286, Phe297, and Tyr341 along with aromatic face-to-face interactions with Trp286 and Tyr341. In addition, our visual inspections proved that all MD snapshots (Figure 5) denoted that isoliquiritigenin still interacted in the AChE active site.

As expected, hydrogen bonds and aromatic interactions were observed using PyPLIF HIPPOS 0.2.0 at simulation time 5 to 10 ns (Supplementary File 3). As also analyzed using visual inspections, all isoliquiritigenin complexes favorably interacted with aromatic amino acid residues, such as Tyr124, Trp286, Phe297, Tyr337, Phe338, and Tyr341. In addition, specific complexes interacted with several other aromatic amino acid residues, such as Tyr72 and Trp86.

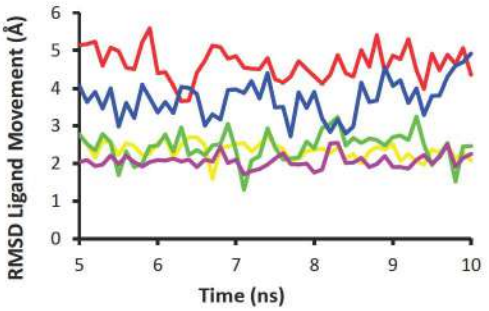

Figure 5. The dynamics conformational changes of isoliquiritigenin interacting with amino acid residues of AChE colored with red (ISL-1), yellow (ISL-2), green (ISL-3), blue (ISL-4), and purple (ISL-5)

The ligand-receptor interactions were also reinforced with hydrogen bonds in all complexes, i.e., Tyr124 (1.96%), Ser293 (1.96%), and Tyr337 (3.92%) for ISL-1. For ISL-2, hydrogen bonds were established with the amino acid residue of Tyr124 as an H-bond donor and acceptor (1.96% and 3.92%) along with His447 (41.17%). In ISL-3 complex, hydrogen bonds also formed only with the amino acid residue of His447 (9.80%), while in the ISL-4 complex, the same hydrogen bond percentage was formed (1.96%) with the amino acid residue of Tyr337 as H-bond donor and acceptor along with Glu202. Subsequently, ISL-5 complex formed hydrogen bonds with aromatic amino acid residue of His447 (21.56%).

As supposed, the hydrogen bonds formation of AChE-isoliquiritigenin stabilization was due to the existence of the hydroxyl moiety attached to the aromatic rings. These findings corresponded closely to the previous research, denoting the importance of the hydroxyl moiety of chalcone derivatives in inhibiting AChE (George et al., 2022). Our SBVS study also proved the existence of p-hydroxyl moiety on the ring attached to carbonyl group of chalcone might serve as the potential lead compound of AChE inhibitor (Riswanto et al., 2017).

The interactions formed of DNP-1 to DNP-5 as well as ISL-1 to ISL-5 were also responsible for the FEB of each MD simulation snapshot (Figure 6). FEB value alterations of donepezil ranged from -9.037 to -12.032 kJ/mol. Those alterations were relatively close to each other complex since there were several overlapped points (Figure 6) (thick line). These FEB analyses denoted that donepezil interacted more favorably than isoliquiritigenin interactions.

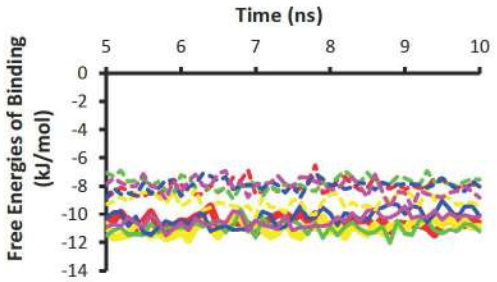

Figure 6. The FEB changes of donepezil (thick line) and isoliquiritigenin (dashed line) with amino acid residues of AChE colored with red (DNP-1 and ISL-1), yellow (DNP-2 and ISL-2), green (DNP-3 and ISL-3), blue (DNP-4 and ISL-4), and purple (DNP-5 and ISL-5)

Notwithstanding that isoliquiritigenin exhibited FEB values ranging from -6.533 to -10.213 kJ/mol, several FEB values from specific MD simulation snapshots appeared lower than those of donepezil. Among ISL-1 to ISL-5, it was noticed that ISL-2 had a lower FEB value, ranging from -8.115 to -10.213 kJ/mol, which indicated more favorable interactions compared to the other isoliquiritigenin complexes. These obtained FEB values were suspected due to the formation of dominant interactions such as hydrogen bond with His447 (41.17%) as previously mentioned,

aromatic face-to-face interactions with Trp86 (96.07%), Phe338 (29.41%), Tyr341 (94.11%), and His447 (29.41%) together with aromatic edge-to-face interactions with Tyr337 (80.39%), Phe338 (78.43%), and His447 (27.45%).

Further dynamics interactions were explored after 10 to 50 ns simulation time. It was observed that donepezil in the DNP-1 to DNP-5 complex possessed maximum RMSD Ligand Movement of 3.540, 2.227, 3.390, 3.466, and 3.199 Å for DNP-1 to DNP-5, respectively whereas the minimum value was still ≤ 2.000 Å. Our visual inspections and PyPLIF HIPPOS 0.2.0 identification proved that donepezil in those complexes remained in the AChE active site, as the interactions are listed (Supplementary File 4). At simulation time of 10 to 50 ns, donepezil in all complexes mainly interacted with Trp86, Trp286, and Tyr341 forming aromatic face-to-face interactions along with Tyr124, Phe297, Tyr337, and Phe338 forming aromatic edge-to-face interactions. Besides, N-benzylpiperidine moiety of donepezil established hydrogen bonds with Tyr337 throughout the simulations. Observable ionic interactions were also found in the DNP-1 and DNP-4 complexes with Asp74.

As predicted, isoliquiritigenin dominantly formed aromatic interactions due to its aromatic moiety (Supplementary File 4). The aromatic interactions were observed with Trp86, Tyr124, Trp286, Phe297, Tyr337, Phe338, and Tyr341 forming aromatic edge-to-face interactions. Thereto, amino acid residues of Trp286, Tyr337, Phe338, and also Tyr341 formed aromatic face-to-face interactions in all AChE-isoliquiritigenin complexes. Hydrogen bonds were also contributed to enhance the molecular interactions, forming with amino acid residues of Tyr124 in all AChE-isoliquiritigenin complexes. These interactions hotspots identifications also proved that even though the RMSD Ligand Movement values at these observed simulations time exceeded 2.000 Å, especially nearly the end of simulations of ISL-2, isoliquiritigenin still interacted with certain amino acid residues in the AChE active site. Hence, these MD simulations could be valuable in incorporating these results to help explain how isoliquiritigenin works to inhibit the AChE activity experimentally.

CONCLUSION

In this work, we proved that isoliquiritigenin acted as an AChE inhibitor through in vitro and in silico studies, verifying the SBVS campaigns in our recently previous study. We discovered that isoliquiritigenin inhibited AChE activity with an IC_{50} value of 126.22 μM, compared to donepezil possessing an IC_{50} value of 36.98 μM. In silico studies revealed from 5 to 10 ns MD simulations, both isoliquiritigenin and donepezil interacted in the AChE active site, stabilized by predominantly aromatic amino acid residues. Further dynamics explorations were observed to 50 ns, verifying that isoliquiritigenin and donepezil still maintained interactions in the AChE active site. Our findings suggest that isoliquiritigenin could be a potential alternative treatment for Alzheimer's disease. This research may also pave the way for further investigation into the effectiveness of natural products containing isoliquiritigenin as the active ingredient.

ACKNOWLEDGMENTS

This research was funded by the Directorate of Research, Technology, and Community Services, the Directorate General of Higher Education, Research, and Technology, the Indonesian Ministry of Education, Culture, Research, and Technology (No. 107/E5/PG.02.00.PL/2024).

CONFLICT OF INTEREST

The authors declare no conflict of interest.

REFERENCES

Ahmed, S., Khan, S. T., Zargaham, M. K., Khan, A. U., Khan, S., Hussain, A., Uddin, J., Khan, A., & Al-Harrasi, A. (2021). Potential therapeutic natural products against alzheimer's disease with reference of acetylcholinesterase. *Biomedicine and Pharmacotherapy*, *139*, 111609. https://doi.org/10.1016/j.biopha.2021.111609

Chen, Y. C. (2015). Beware of docking! *Trends in Pharmacological Sciences*, *36*(2), 78–95. https://doi.org/10.1016/J.TIPS.2014.12.001

Cho, J. K., Ryu, Y. B., Curtis-Long, M. J., Ryu, H. W., Yuk, H. J., Kim, D. W., Kim, H. J., Lee, W. S., & Park, K. H. (2012). Cholinestrase inhibitory effects of geranylated flavonoids from Paulownia tomentosa fruits. *Bioorganic & Medicinal Chemistry*, *20*(8), 2595–2602. https://doi.org/10.1016/j.bmc.2012.02.044

Diallo, B. N., Swart, T., Hoppe, H. C., Tastan Bishop, Ö., & Lobb, K. (2021). Potential repurposing of four FDA approved compounds with antiplasmodial activity identified through

proteome scale computational drug discovery and in vitro assay. *Scientific Reports*, *11*(1), 1–15. https://doi.org/10.1038/s41598-020-80722-2

Dong, M., Yang, Z., Gao, Q., Deng, Q., Li, L., & Chen, H. (2024). Protective effects of isoliquiritigenin and licochalcone B on the immunotoxicity of BDE-47: antioxidant effects based on the activation of the Nrf2 pathway and inhibition of the NF-κB pathway. *Antioxidants*, *13*(4), 445. https://doi.org/10.3390/antiox13040445

Gajendra, K., Pratap, G. K., Poornima, D. V., Shantaram, M., & Ranjita, G. (2024). Natural acetylcholinesterase inhibitors: A multi-targeted therapeutic potential in alzheimer's disease. *European Journal of Medicinal Chemistry Reports*, *11*(100154). https://doi.org/10.1016/j.ejmcr.2024.100154

Gaur, R., Yadav, K. S., Verma, R. K., Yadav, N. P., & Bhakuni, R. S. (2014). In vivo anti-diabetic activity of derivatives of isoliquiritigenin and liquiritigenin. *Phytomedicine*, *21*(4), 415–422. https://doi.org/10.1016/j.phymed.2013.10.015

George, G., Koyiparambath, V. P., Sukumaran, S., Nair, A. S., Pappachan, L. K., Al-Sehemi, A. G., Kim, H., & Mathew, B. (2022). Structural modifications on chalcone framework for developing new class of cholinesterase inhibitors. *International Journal of Molecular Sciences*, *23*(3121). https://doi.org/10.3390/ijms23063121

Hafiz, Z. Z., Amin, M. 'Afif M., James, R. M. J., Teh, L. K., Salleh, M. Z., & Adenan, M. I. (2020). Inhibitory effects of raw-extract Centella asiatica (RECA) on acetylcholinesterase, inflammations, and oxidative stress activities via in vitro and in vivo. *Molecules*, *25*(1), 892.

Istyastono, E. P., Yuniarti, N., Prasasty, V. D., Mungkasi, S., Waskitha, S. S. W., Yanuar, M. R. S., & Riswanto, F. D. O. (2023). Caffeic acid in spent coffee grounds as a dual inhibitor for MMP-9 and DPP-4 enzymes. *Molecules*, *28*, 7182. https://doi.org/10.3390/molecules28207182

Ketenci, S., Acet, N. G., Sarıdoğan, G. E., Aydın, B., Cabadak, H., & Gören, M. Z. (2020). The neurochemical effects of prazosin treatment on fear circuitry in a rat traumatic stress model. *Clinical Psychopharmacology and Neuroscience*, *18*(2), 219–230. https://doi.org/10.9758/cpn.2020.18.2.219

Khan, M. T. H., Orhan, I., Şenol, F. S., Kartal, M., Şener, B., Dvorská, M., Šmejkal, K., & Šlapetová, T. (2009). Cholinesterase inhibitory activities of some flavonoid derivatives and chosen xanthone and their molecular docking studies. *Chemico-Biological Interactions*, *181*(3), 383–389. https://doi.org/10.1016/j.cbi.2009.06.024

Kim, J. Y., Lee, W. S., Kim, Y. S., Curtis-long, M. J., Lee, B. W., Ryu, Y. B., & Park, K. H. (2011). Isolation of cholinesterase-inhibiting flavonoids from Morus lhou. *Journal of Agricultural and Food Chemistry*, *59*(9), 4589–4596.

Konrath, E. L., Passos, C. D. S., Klein-Júnior, L. C., & Henriques, A. T. (2013). Alkaloids as a source of potential anticholinesterase inhibitors for the treatment of alzheimer's disease. *Journal of Pharmacy and Pharmacology*, *65*(12), 1701–1725. https://doi.org/10.1111/jphp.12090

Li, H., Ye, M., Zhang, Y., Huang, M., Xu, W., Chu, K., Chen, L., & Que, J. (2015). Blood-brain barrier permeability of Gualou guizhi granules and neuroprotective effects in ischemia/reperfusion injury. *Molecular Medicine Reports*, *12*(1), 1272–1278. https://doi.org/10.3892/mmr.2015.3520

Liu, K., & Kokubo, H. (2017). Exploring the stability of ligand binding modes to proteins by molecular dynamics simulations: a cross-docking study. *Journal of Chemical Information and Modeling*, *57*(10), 2514–2522. https://doi.org/10.1021/ACS.JCIM.7B00412/SUPPL_FILE/CI7B00412_SI_001.PDF

Liu, K., Watanabe, E., & Kokubo, H. (2017). Exploring the stability of ligand binding modes to proteins by molecular dynamics simulations. *Journal of Computer-Aided Molecular Design*, *31*(2), 201–211. https://doi.org/10.1007/s10822-016-0005-2

Mahmood, N. D., Nasir, N. L. M., Rofiee, M. S., Tohid, S. F. M., Ching, S. M., Teh, L. K., Salleh, M. Z., & Zakaria, Z. A. (2014). Muntingia calabura: A review of its traditional uses, chemical properties, and pharmacological observations. *Pharmaceutical Biology*,

52(12), 1598–1623. https://doi.org/10.3109/13880209.2014.908397

Mohsin, N. U. A., & Ahmad, M. (2020). Donepezil: A review of the recent structural modifications and their impact on anti-alzheimer activity. *Brazilian Journal of Pharmaceutical Sciences*, *56*(e18325), 1–16. https://doi.org/10.1590/S2175-97902019000418325

Nichols, E., Steinmetz, J. D., Vollset, S. E., Fukutaki, K., Chalek, J., Abd-Allah, F., Abdoli, A., Abualhasan, A., Abu-Gharbieh, E., Akram, T. T., Al Hamad, H., Alahdab, F., Alanezi, F. M., Alipour, V., Almustanyir, S., Amu, H., Ansari, I., Arabloo, J., Ashraf, T., … Vos, T. (2022). Estimation of the global prevalence of dementia in 2019 and forecasted prevalence in 2050: an analysis for the global burden of disease study 2019. *The Lancet Public Health*, *7*(2), e105–e125. https://doi.org/10.1016/S2468-2667(21)00249-8

Ramalingam, M., Kim, H., Lee, Y., & Lee, Y. Il. (2018). Phytochemical and pharmacological role of liquiritigenin and isoliquiritigenin from radix glycyrrhizae in human health and disease models. *Frontiers in Aging Neuroscience*, *10*(November), 1–15. https://doi.org/10.3389/fnagi.2018.00348

Riswanto, F. D. O., Hariono, M., Yuliani, S. H., & Istyastono, E. P. (2017). Computer-aided design of chalcone derivatives as lead compounds targeting acetylcholinesterase. *Indonesian Journal of Pharmacy*, *28*(2), 100–111. https://doi.org/10.14499/indonesianjpharm28iss2pp100

Riswanto, F. D. O., Waskitha, S. S. W., Yanuar, M. R. S., & Enade. (2024). *Structure-based virtual screening on a new open-source natural products database LOTUS to discover acetylcholinesterase ınhibitors*. *28*(4), 1099–1106. https://dx.doi.org/10.29228/jrp.792

Shi, D., Yang, J., Jiang, Y., Wen, L., Wang, Z., & Yang, B. (2020). The antioxidant activity and neuroprotective mechanism of isoliquiritigenin. *Free Radical Biology and Medicine*, *152*, 207–215. https://doi.org/10.1016/j.freeradbiomed.2020.03.016

Sugimoto, H. (1999). Structure-activity relationships of acetylcholinesterase inhibitors: Donepezil hydrochloride for the treatment of alzheimer's disease. *Pure and Applied Chemistry*, *71*(11), 2031–2037. https://doi.org/10.1351/pac199971112031

Wang, K. L., Yu, Y. C., & Hsia, S. M. (2021). Perspectives on the role of isoliquiritigenin in cancer. *Cancers*, *13*(15), 1–37. https://doi.org/10.3390/CANCERS13010115

Waskitha, S. S. W., Istyastono, E. P., & Riswanto, F. D. O. (2023). Molecular docking study of caffeic acid as acetylcholinesterase inhibitor. *Journal of Food and Pharmaceutical Sciences*, *11*(3), 867–873. https://doi.org/10.22146/jfps.7665

Windah, A. L. L., & Istyastono, E. P. (2024). Computational studies of donepezil and acetylcholinesterase molecular dynamics interactions. *Journal of Pharmaceutical Sciences and Community, 21*(1), 91–99.

Zhang, X., Yeung, E. D., Wang, J., Panzhinskiy, E. E., Tong, C., Li, W., & Li, J. (2010). Isoliquiritigenin, a natural anti-oxidant, selectively inhibits the proliferation of prostate cancer cells. *Clinical and Experimental Pharmacology and Physiology*, *37*(8), 841–847. https://doi.org/10.1111/j.1440-1681.2010.05395.x